International Journal of Minerals, Metallurgy and Materials
Volume 23, Number 7, July 2016, Page 731
DOI: 10.1007/s12613-016-1287-z

Kinetic approach to the study of froth flotation applied to a lepidolite ore

Nathália Vieceli[1)], *Fernando O. Durão*[2)], *Carlos Guimarães*[2)], *Carlos A. Nogueira*[3)], *Manuel F. C. Pereira*[2)], *and Fernanda Margarido*[1)]

1) Center for Innovation, Technology and Policy Research - IN+, Instituto Superior Técnico, University of Lisbon, 1049-001 Lisboa, Portugal
2) CERENA - Centro de Recursos Naturais e Ambiente, DECivil, Instituto Superior Técnico, University of Lisbon, 1049-001 Lisboa, Portugal
3) LNEG - Laboratório Nacional de Energia e Geologia, I.P., Campus do Lumiar, 1649-038 Lisboa, Portugal
(Received: 29 November 2015; revised: 24 December 2015; accepted: 29 December 2015)

Abstract: The number of published studies related to the optimization of lithium extraction from low-grade ores has increased as the demand for lithium has grown. However, no study related to the kinetics of the concentration stage of lithium-containing minerals by froth flotation has yet been reported. To establish a factorial design of batch flotation experiments, we conducted a set of kinetic tests to determine the most selective alternative collector, define a range of pulp pH values, and estimate a near-optimum flotation time. Both collectors (Aeromine 3000C and Armeen 12D) provided the required flotation selectivity, although this selectivity was lost in the case of pulp pH values outside the range between 2 and 4. Cumulative mineral recovery curves were used to adjust a classical kinetic model that was modified with a non-negative parameter representing a delay time. The computation of the near-optimum flotation time as the maximizer of a separation efficiency (SE) function must be performed with caution. We instead propose to define the near-optimum flotation time as the time interval required to achieve 95%–99% of the maximum value of the SE function.

Keywords: lepidolite; lithium ore treatment; froth flotation; kinetic analysis

1. Introduction

Flotation, specifically froth flotation, represents an important mineral concentration process. It has attracted much attention from researchers, with flotation models being used since the early 1930s. However, because of the complexity of the flotation process and technological limitations, most of the existing models have not been perfected. Nonetheless, the quantification of kinetic parameters has resulted in improvements in the industrial flotation process by providing information about the process rate [1]. One of the main advantages of the use of modeling and simulation techniques in the development of flotation circuits is cost reductions. Furthermore, several contributions have been directed to the development of models to describe ore floatability [2].

Lithium was discovered in 1817, and its major applications are in the manufacture of glass, ceramics, and lubricating greases. Currently, it is mainly used in the pharmaceutical and high-tech industries because of its numerous applications, which include rechargeable batteries and electronic components [3]. Moreover, since 1990, when lithium-ion rechargeable batteries were first commercialized by Sony, lithium has become essential for modern industry. It is regarded as a strategic metal, widely employed in various portable electronic devices because of its high energy density and long cycle life. Lithium extraction has thus become a high priority [4].

Lithium is generally extracted from minerals found in igneous rocks and from lithium chloride salts found in brine pools. Other resources containing this metal, including low-grade ores, are ignored [5]. Although lithium is present in approximately 145 mineral species, only spodumene, lepidolite, petalite, amblygonite, and eucryptite are the object of commercial exploration of lithium [6]. The demand for this metal has increased, as has research focused on optimizing its extraction from low-grade ores; however, studies on the kinetics of the lithium mineral concentration stage by flotation have not yet been reported in the literature.

Corresponding author: Nathália Vieceli E-mail: nathalia.vieceli@tecnico.ulisboa.pt

Producing high-grade lithium concentrates for metallurgical processing requires exploitation of the physical properties that differentiate lithium minerals from the gangue mineral associated with them. An analysis of the technology employed in large mining plants reveals that froth flotation remains a critical process in the production of high-purity lithium mineral concentrates [7].

Portugal occupies an important position in the ranking of lithium production, mainly because of the exploitation of pegmatite aplite veins, from which lithium is extracted, predominantly as lepidolite. The area of Gonçalo-Vela (Guarda District) contains the largest lepidolite reserves in Portugal [8]. The estimated total volume of the minimum gross geological reserves of lithium ore in the Gonçalo–Seixo Amarelo area is larger than 544100 m^3; given that the specific gravity of the lithium ore is 2.6, this volume corresponds to more than 1400000 t [9]. Portuguese lepidolites also contain, in addition to lithium, substantial amounts of rubidium, another valuable metal that should not be disregarded.

In Portugal, lithium has been used mainly in the glass and ceramics industries, where its usefulness has been recognized for several years, especially in the reduction of the melting point of ceramic pastes [10]. However, despite the existence of large reserves of lithium ores, lithium concentrates are not produced in Portugal. As a starting point for a full optimization study of the flotation operating conditions, we here present the results of a set of experimental tests whose main objectives were to evaluate and compare the selectivity of alternative cationic flotation collectors, define a range of suitable pulp pH values, and estimate the near-optimum flotation time of a lepidolite ore. A kinetics approach is used to achieve these objectives.

2. Kinetic models applied to batch flotation

Flotation kinetics can be described macroscopically by a first-order rate equation [11], although a second-order rate model is also often considered. Thus, by analogy to the differential equation of the kinetics of chemical reactions, the general equation of the kinetic model for flotation can be written as

$$\frac{\mathrm{d}\,m(t)}{\mathrm{d}\,t} = -km(t)^n, \tag{1}$$

where $m(t)$ represents the mass of floatable mineral at time instant t and n is an exponent defining the order of the kinetic equation, typically ranging from 0 to 2.

Several models have been developed and, according to Lynch *et al.* [12] and Yuan *et al.* [13], they can be classified into three categories: empirical models, probabilistic models, and kinetic models. The empirical models are too specific, considering only data in the range of conditions where they were applied and usually involving a trial-and-error approach, whereas probability models, with certain constraints, can be reduced to kinetic models.

For mono-sized particles of a given mineral group with a well-defined flotation rate constant k and first-order kinetics, the time change of the mass, $m(t)$, of such particles in a semi-batch flotation system is given by

$$\frac{\mathrm{d}\,m(t)}{\mathrm{d}\,t} = -km(t), \text{ with initial condition } m(0) = R_\infty m_0 \tag{2}$$

where m_0 is the initial mass of mineral particles and $R_\infty m_0$ is the initial mass of the floatable mineral particles. The solution function of $m(t)$ is given by

$$\begin{aligned} m(t) &= m(0)\exp(-kt) \\ &= R_\infty m_0 \exp(-kt). \end{aligned} \tag{3}$$

The recovery in the floated product is, by definition, computed as

$$\begin{aligned} R(t) &= \frac{R_\infty m_0 - m(t)}{m_0} \\ &= \frac{R_\infty m_0 - R_\infty m_0 \exp(-kt)}{m_0} \\ &= R_\infty - R_\infty \exp(-kt) \\ &= R_\infty \left[1 - \exp(-kt)\right] \end{aligned} \tag{4}$$

The model parameter, R_∞, can be interpreted as the ultimate/limit recovery; it refers to the mineral recovery after a very long flotation time. For cases with a rate-constant distribution, the general model can be written as

$$R(t) = R_\infty \left[1 - \int_0^\infty f(k)\exp(-kt)\,\mathrm{d}\,k\right] \tag{5}$$

if k is a continuous parameter and as

$$R(t) = R_\infty \left[1 - \sum_{k_i} f(k_i)\exp(-k_i t)\right] \tag{6}$$

if k is a discrete parameter. Some well-known model variants have been proposed in the literature [12–16]. A recent review of first-order flotation kinetic models has also been published [17].

3. Experimental

3.1. Materials and reagents

The material used in this work, lepidolite ore, originated from Gonçalo–Seixo Amarelo, situated in Guarda District, Portugal, and was kindly provided by Felmica Minerais In-

dustriais, S.A. (MOTA® Ceramic Solutions). Samples for flotation tests were prepared through successive stages of screening and fine crushing in a roll crusher (Sturtevant). The objective was to obtain a flotation feed with a minimum amount of very fine particles and a maximum particle size of 500 μm. This maximum size of 500 μm is, indeed, the upper limit of application of the froth flotation operation for materials with a specific gravity of approximately 2.6–2.7 (the upper limit is commonly stated as 300 μm) [18]. The fine crushed material was then submitted to division with a riffle sample splitter, which provided samples of approximately 750 g. This sample mass was considered taking into account the minimal representative mass of ore required.

Particle size analysis was performed by the dry sieving method. The mineralogical characterization was conducted by X-ray powder diffraction (XRPD, PANanalytical X'PERT-PRO diffractometer) to identify the main mineral phases present in the sample. XRPD analysis was carried out using Cu K_α radiation and a scan step size of 0.050° (2θ), a step time of 150 s, and generator settings of 35 mA and 40 kV. The X'PERT HIGHSCORE PLUS software, in conjunction with the PDF4 database, was used to analyze the data.

Photographs of the original sample and of the fine crushed sample (−500 μm) used in the flotation tests are shown in Fig. 1.

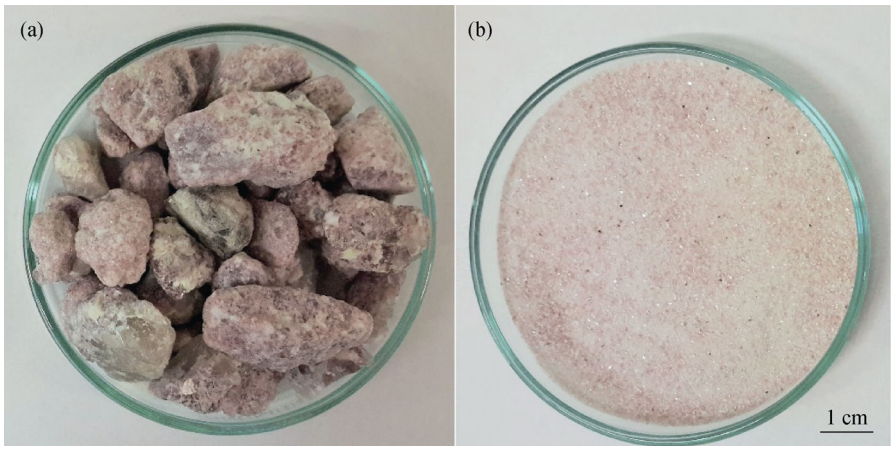

Fig. 1. Original sample (a) and fine crushed sample (b) employed in the flotation tests.

Two flotation collectors were tested in this study, an Aeromine 3000C and an Armeen 12D, which were kindly supplied by Cytec and Akzo Nobel, respectively. The Aeromine 3000C was tested as a non-diluted solution (5vol% in water), as proposed in the *Mining Chemicals Handbook* [19], whereas the collector Armeen 12D was added as a solution (5vol%) in ethanol because it is not soluble in water. We also tested two collector dosages (350 and 500 $g \cdot t^{-1}$) based on the recommendations for these flotation collectors.

The pulp pH value was controlled by the addition of diluted solutions of sulfuric acid (H_2SO_4) and sodium hydroxide (NaOH) (10vol% in both cases). The reagents used were of analytical grade (Merck), and the solutions were prepared using demineralized water.

4-methyl-2-pentanol (MIBC, 98%) from Sigma-Aldrich was used as a frother agent. According to Ref. [20], this frother produces a more open froth, which allows good drainage of the entrained gangue minerals, improving the selectivity of the process. Moreover, being an alcohol, it tends to form a thin film on the bubbles, thus carrying less water and reducing slime entrainment (ultrafine particles).

3.2. Methodology

3.2.1. Desliming step

A desliming (slimes removal) step was performed in some tests, before the flotation operation, because of the high consumption of reagents by very fine particles and because of their high surface area. This operation was carried out through the "beaker decantation" procedure, as described by Wills and Munn [21], as a sedimentation method for particle size analysis. By combining solid particle sedimentation in a diluted pulp and siphoning off the decanted (supernatant water and solids), a removal efficiency of at least 75% of the particles with a size finer than 30 μm (corresponding to one-half of the separation diameter of 60 μm) is possible using three decantation cycles. The choice of the separation diameter was supported by the results of both the particle size analysis and the XRPD analysis. The height of the immersed siphon tube and the sedimentation time were estimated using the settling velocity equations for spherical particles, as presented in Refs. [22–23].

3.2.2. Flotation tests

The flotation tests were performed using a Leeds labora-

tory flotation cell with a volume of 3.0 L. An air compressor was used to inject air into the pulp in the flotation cell. The impeller rotation speed and the air flow rate were kept constant at 750 r·min^{-1} and 200 L·h^{-1}, respectively. A stopwatch was used to monitor the time. The conditioning time was fixed at 10 min. The pulp density was set at 50wt% of solids. During the flotation tests, the pulp density was adjusted to 25wt% of solids, which is considered a suitable value according to Ref. [24]. The pulp–froth interface and the pulp pH value were kept constant during the tests by the addition of a sufficient volume of water whose pH value was regulated according to the pulp pH value of the flotation test when required. Concentrates were collected at different specific flotation time to provide the required data to support the study of the flotation kinetics and the adjustment of the parameters of the kinetic model. The conditioning time after addition of the collector ranged from 5 to 8 min.

The pulp pH values were tested on the basis of the recommendations for the evaluated collectors. According to Ref. [19], the Aeromine 3000C can be used for the flotation of mica in either acid or alkaline media. Given this wide range of application, we also investigated flotation in neutral pH values because operations in this pH range could be interesting given the associated safety and environmental benefits. The pulp pH value was measured using a previously calibrated pH meter (Eutech Instruments, Ion 510). The experimental conditions of the four flotation tests performed are summarized in Fig. 2.

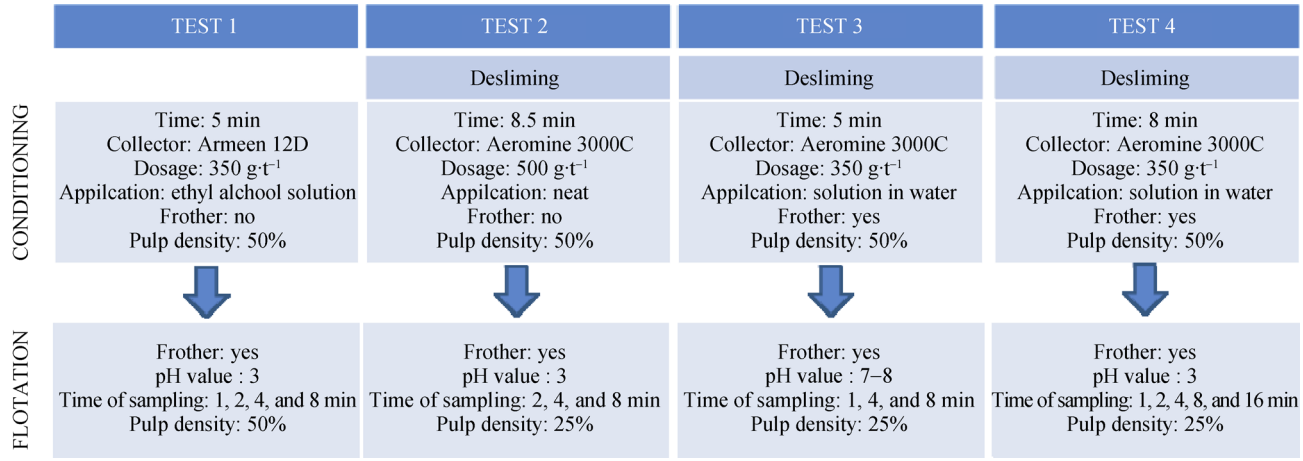

Fig. 2. Experimental operating conditions of the flotation tests.

3.3. Chemical analysis and recovery determination

Products obtained during the tests were filtered (Whatman, ϕ125 mm, ashless), dried in an oven with air circulation (Memmert) for 24 h at 80°C, and further sampled for chemical analysis, which was performed by acid digestion in a microwave oven (CEM MDS-2000). The measurement of lithium and rubidium contents was carried out by atomic absorption (AA) spectrometry (SOLAR 969 AA spectrometer, Thermo Elemental).

The recovery, as a function of the flotation time, of the lepidolite in the floated product was determined by measuring the lithium content and assuming that lepidolite has a lithium content of 3wt%. For the recovery of the gangue minerals in the floated product, the content was taken as the complement to 100% of the lepidolite content.

4. Flotation kinetics modeling

The test results were used to adjust the first-order kinetics equation modified by Wills and Munn [21] and by Agar [25]. These authors proposed the incorporation of a correction parameter for the flotation time because, in batch flotation tests, some hydrophobic solids may be attached to air bubbles formed during the conditioning time, thereby resulting in a faster flotation than would naturally occur. This faster flotation, in turn, causes a positive correction to time zero because flotation starts before the introduction of the air flow. However, when the air flow starts, several seconds pass before a full depth of loaded froth is formed in the cell, giving a negative correction to time zero. The proposed modified rate equation for batch flotation tests is as follows:

$$R(t) = R_{\infty}\left\{1-\exp\left[-k\left(t+b\right)\right]\right\} \tag{7}$$

where $R(t)$ is the cumulative recovery after the flotation time t, t is the cumulative flotation time, R_{∞} is the maximum theoretical flotation recovery, b is the parameter for the correction of the flotation starting time, and k is the first-order rate constant (min^{-1}) [21]. However, in the tests performed, the delay effect of flotation was quite pronounced; conse-

quently, we decided to slightly modify the model proposed by Agar [25], reflecting the interpretation of the time correction, b, as a non-negative delay time. The kinetic model with a non-negative delay time, b, can be rewritten as

$$R_X(t) = \max\left(0, R_{\infty,X}\left\{1-\exp\left[-k_X(t-b)\right]\right\}\right) = \begin{cases} 0, & t < b \\ R_{\infty,X}\left\{1-\exp\left[-k_X(t-b)\right]\right\}, & t \geq b \end{cases} \quad (8)$$

where X = M (mineral of interest) or G (gangue) and $b \geq 0$.

The mineral composition of the lithium ore consists mainly of lepidolite (lithium-bearing mineral), quartz, and feldspar minerals. Because the flotation behaviors of these last two minerals are similar, they can be combined into a single mineral group referred to hereafter as gangue. These two mineral groups (lepidolite and gangue) are essentially liberated from each other, in the case of a maximum particle size of 500 μm.

For each mineral group, the three parameters of the kinetic flotation model were adjusted by solving a non-linear parameter estimation problem consisting of the minimization of the sum of squares of residues (SQR) subject to simple bound constraints. The residues are the differences between the recoveries measured in the flotation tests for the mineral of interest, lepidolite (R_M), or for the associated gangue minerals (R_G), and the corresponding recoveries predicted by the model. The non-linear bound constrained optimization problem posed by the parameter estimation problem was solved by a robust and efficient generalized reduced gradient (GRG) algorithm provided as an add-in called *Solver* for the EXCEL® application.

Notably, because the flotation of both groups of minerals occurs together, we should ensure that both are subject to the same delay time. In this way, when the obtained delay time differed between the mineral groups, parameter b was adjusted to become a common value.

The constrained optimization problem is summarized as

$$\min_{\{R_{\infty,X},\, k_X,\, b_X\}} \mathrm{SQR} = \sum_{j=1}^{n}\left[R_X\left(t_j \mid R_{\infty,X}, k_X, b_X\right) - R_X^{\mathrm{obs}}\left(t_j\right)\right]^2$$

subject to :

$$\begin{aligned} 0 \leq R_{\infty,X} \leq 100 \\ b_{\min} \leq b_X \leq b_{\max} \\ K_X \geq 0 \end{aligned} \quad (9)$$

where n is the number of collected floated increments, $R_X\left(t_j \mid R_{\infty,X}, k_X, b_X\right)$ is the recovery predicted by the kinetic model for flotation time t_j and by given values of model parameters, and $R_X^{\mathrm{obs}}\left(t_j\right)$ is the corresponding measured recovery.

Using the adjusted parameters of the kinetic model, we can estimate the optimum flotation time, t_{opt}, which is the time that maximizes the separation efficiency function, SE(t), defined in Eq. (10) as the difference of the cumulative recoveries between lepidolite and the gangue minerals:

$$\mathrm{SE}(t) = R_M(t) - R_G(t) \quad (10)$$

A closed-form solution to compute the optimum flotation time can be obtained by finding the zero of the first-order derivative of the separation efficiency function with respect to time t (i.e., the first-order necessary condition of the unconstrained optimization).

Solving the first-order necessary condition for an unconstrained maximum of function SE(t) with respect to t_{opt} gives Eq. (11):

$$\left.\frac{\mathrm{d}\,\mathrm{SE}(t)}{\mathrm{d}\,t}\right|_{t=t_{\mathrm{opt}}} = 0 \Rightarrow t_{\mathrm{opt}} = \frac{\left[\ln\left(\frac{R_{\infty,M}k_M}{R_{\infty,G}k_G}\right) - b_M k_M + b_G k_G\right]}{\left(k_M - k_G\right)} \quad (11)$$

The solution of Eq. (11) must always be checked because the optimum flotation time value is not necessarily non-negative (i.e., k_M may be less than k_G) and is not necessarily the maximizer. The application of Eq. (11) also assumes that the separation efficiency function (curve) achieves a unique well-defined maximum value, which is generally not true because the time range tested is not sufficiently long or because the recovery curves become almost parallel. In the latter case, if the values for the ultimate/limit recoveries are assumed to be significantly different, the maximum separation efficiency is equal to $R_{\infty,M} - R_{\infty,G}$, which is an asymptotic value that is achieved theoretically for a very long flotation time. A better approximation to the near-optimum flotation time can then be defined as the interval of the flotation time required to achieve a value of 95% to 99% of the maximum separation efficiency; that is, 95% to 99% of $R_{\infty,M} - R_{\infty,G}$. The flotation times, t_{95} and t_{99}, required to achieve 95% and 99% of the maximum separation efficiency, respectively, are the solutions of the following non-linear Eq. (12), with β = 95 or 99:

$$R_M(t) - R_G(t) - \frac{\beta}{100}\left(R_{\infty,M} - R_{\infty,G}\right) = 0 \quad (12)$$

In case of equal or very similar ultimate/limit recoveries, the aforementioned flotation times, t_{95} and t_{99}, can still be estimated using Eq. (13):

$$R_M(t) - R_G(t) - \frac{\beta}{100}\mathrm{SE}\left(t_{\mathrm{opt}}\right) = 0 \quad (13)$$

where the difference $R_{\infty,M} - R_{\infty,G}$ is replaced by the optimal value of the separation efficiency function obtained for

the flotation time equal to t_{opt}.

5. Results and discussion

The results of the particle size analyses, as well as the lithium and rubidium contents in each size fraction, are summarized in Table 1. As patent in Table 1, the highest lithium and rubidium contents were observed for the particle size range −125 μm+90 μm (1.53wt% and 0.32wt%, respectively) and the lowest ones were observed for size fraction −32 μm (0.89wt% and 0.20wt%, respectively).

The lithium and rubidium contents are greater in the coarser size fractions (−250 μm+63 μm), as shown in the characterization results presented in Table 1. The authors of previous studies [26–28] reported a higher content in the coarser size fraction. According to Nogueira [28], the coarser size range is richer in lithium because of the lamellar structure of micas, where lithium occurs. The comminution of the lamellar structures is very difficult; thus, lepidolite distributes predominantly in this particle size fraction. The different results obtained in this study could be related to the presence of mixed (non-liberated) particles in the coarser size fraction. The lowest value of lithium in the case of the finer fraction could be due to the preferential concentration of clay and Na feldspar particles, in the last case, in close relation to its perfect cleavage.

Table 1. Particle size distribution and contents of rubidium and lithium

Particle size / μm	Corrected / wt%	Cumulative under size / %	Li content* / wt%	Li distribution / %	Rb content* / wt%	Rb distribution / %
−500+355	22.79	100.00	1.14	19.60	0.31	16.58
−355+250	16.07	77.21	1.31	15.78	0.35	15.25
−250+180	19.87	61.13	1.41	21.01	0.39	21.86
−180+125	13.03	41.26	1.52	14.89	0.43	16.75
−125+90	10.29	28.23	1.53	11.85	0.32	13.43
−90+63	7.19	17.94	1.46	7.88	0.29	8.50
−63+45	3.97	10.75	1.31	3.90	0.27	3.78
−45+32	2.28	6.78	1.22	2.08	0.23	1.87
−32	4.50	4.50	0.89	3.01	0.20	1.98
Total / Average (raw feed)	100.00	—	1.33	100.00	0.34	100.00

Note: *Corrected values.

Lepidolite, quartz, and Na feldspar (albite) are the main mineral phases, as evident from the XRPD patterns (Fig. 3).

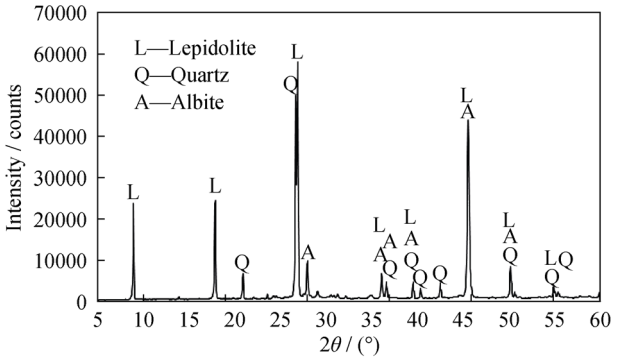

Fig. 3. XRPD pattern of the lepidolite raw feed ore. Only major reflections are shown.

The main results of the flotation tests are shown in Table 2, along with the ratio between the lithium and rubidium contents. The observed cumulative recoveries are plotted against the flotation time for the lepidolite and the gangue minerals in Figs. 4 and 5, along with the corresponding recoveries predicted through the kinetic model.

As manifest in Fig. 4(a), the flotation in Test 1 was very selective, resulting in substantial differences between the recoveries of lepidolite and gangue minerals. As shown in Table 2, the non-floated material contained only 0.38wt% Li. We also verified that the flotation time of Test 1 could be increased to 10 or 12 min because the lithium content of 2.36wt% of the incremental concentrate collected after 8 min of flotation was much higher than the lithium content of the feed. Moreover, with respect to the average content of lithium and rubidium in the floated fractions, a concentrate with lithium and rubidium contents 1.73 and 1.58 times richer than those of the feed, respectively, was obtained in Test 1, along with a non-floated product with 0.38wt% Li and 0.11wt% Rb (corresponding to lithium and rubidium recoveries of 79.47% and 74.24%, respectively).

Table 2. Main results of the flotation tests

Test No.	Product	Mass / %	Li content / wt%	Li recovery / %	Rb content / wt%	Rb recovery / %	Li/Rb mass ratio
1	(Raw) feed	100.00	1.33	100.00	0.34	100.00	3.90
	Floated 1 min	5.02	2.29	8.66	0.50	7.36	4.60
	Floated 2 min	15.61	1.91	22.43	0.54	24.51	3.57
	Floated 4 min	11.45	2.63	22.65	0.59	19.95	4.43
	Floated 8 min	14.52	2.36	25.72	0.53	22.42	4.48
	Non-floated	47.48	0.38	13.47	0.11	15.38	3.42
	Losses	5.90					
2	(Raw) feed	100.00	1.33	100.00	0.34	100.00	3.90
	Desliming	10.13	1.05	8.03	0.29	8.58	3.65
	(Flotation) feed	89.87	1.36	91.97	0.35	91.42	3.93
	Floated 2 min	3.93	2.63	7.78	0.58	6.71	4.53
	Floated 4 min	8.33	2.74	17.17	0.62	15.21	4.40
	Floated 8 min	21.57	2.52	40.85	0.54	34.36	4.64
	Non-floated	53.33	0.71	28.60	0.21	33.44	3.34
	Losses	2.72					
3	(Raw) feed	100.00	1.33	100.00	0.34	100.00	3.90
	Desliming	10.54	1.09	8.65	0.31	9.54	3.54
	(Flotation) feed	89.46	1.36	91.35	0.34	90.46	3.94
	Floated 1 min	23.94	1.62	29.22	0.49	34.28	3.33
	Floated 4 min	34.99	1.43	37.68	0.44	45.00	3.27
	Floated 8 min	8.85	1.23	8.17	0.40	10.32	3.09
	Non-floated	18.70	0.91	12.84	0.25	13.89	3.61
	Losses	2.99					
4	(Raw) feed	100.00	1.33	100.00	0.34	100.00	3.90
	Desliming	9.74	0.55	4.05	0.12	3.52	4.49
	(Flotation) feed	90.26	1.41	95.95	0.36	96.48	3.88
	Floated 1 min	10.91	2.54	20.86	0.52	16.70	4.87
	Floated 2 min	10.87	2.82	23.08	0.57	18.30	4.92
	Floated 4 min	13.66	2.65	27.22	0.68	27.27	3.90
	Floated 8 min	4.52	2.49	8.48	0.55	7.25	4.56
	Floated 16 min	1.09	2.10	1.72	0.48	1.53	4.38
	Non-floated	47.65	0.37	13.37	0.08	11.24	4.64
	Losses	1.56					

Notably, although a selective flotation using the collector Armeen 12D was observed, its application encounters some limitations because it is not soluble in water and is therefore added as a solution in ethyl alcohol. Alcohols have frother properties, and although these properties may lead to a reduction of reagent consumption, they may also introduce difficulties with respect to controlling the froth during the process. The results obtained through the kinetic model appear to fit the experimental data well, both for lepidolite and for the gangue minerals (Fig. 4(a)). Notably, losses during Test 1 were not substantial, as shown in Table 2.

Although a different collector was used in Test 2 and was applied non-diluted, Fig. 4(b) reveals that the conditions in this test enhanced the selective flotation; a difference in recoveries between lepidolite and gangue minerals is evident. Like in the first test (Test 1), the flotation time in the second test (Test 2) could be increased to 12 min because the lithium content in the incremental concentrate at 8 min of flotation (2.52wt%) is still higher than that in the feed (1.33wt%), as shown in Table 2. However, with respect to the average content of lithium and rubidium in the floated fractions of Test 2, concentrates 1.93 and 1.68 times richer than the feed

were obtained. The cumulative recovery in the floated fraction was 71.54% for lithium and 56.28% for rubidium. The non-floated fraction contained 0.71wt% Li and 0.21wt% Rb.

The introduction of the desliming step removed 10% to 10.5% of the initial sample mass, with lithium losses totaling 8% to 8.5% (Table 2). The test losses of approximately 3% are considered acceptable. The results obtained through the kinetic model appear to better fit the experimental values of the gangue recovery than the experimental values of the lepidolite recovery, as shown in Fig. 4(b).

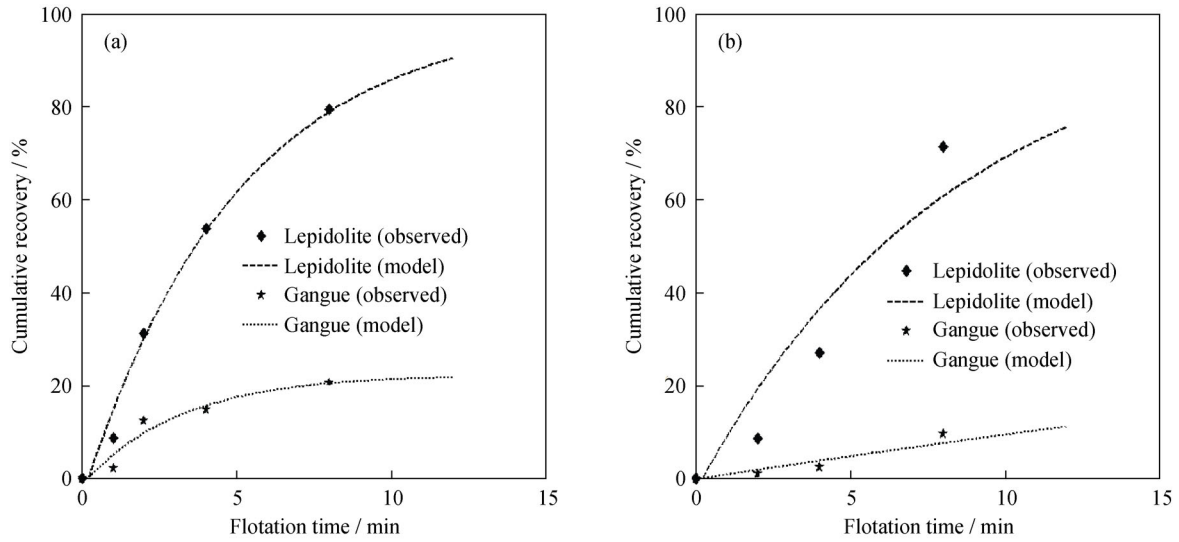

Fig. 4. Cumulative recovery experimentally observed and predicted by the model versus flotation time: (a) Test 1; (b) Test 2.

In the case of Test 3 (Fig. 5(a)), the flotation separation was weakly selective. We verified this result by comparing the recovery curves of lepidolite and gangue minerals, which are similar and almost parallel. This result may indicate that selectivity depends on the pH value of the pulp; in this case, a neutral value (the natural water pH value) appears to adversely influence the process.

According to the electrostatic model of flotation [29–32], which is the most commonly used model to explain the adsorption of the cationic collector molecules on oxides and silicate mineral surfaces, these species are adsorbed through physical interaction and act as counter-ions in the Stern layer of the electric double layer at the interface mineral/aqueous solution. The physical interaction is controlled by the electrical nature (sign) of the mineral surface, which is strongly related to the pH value. The pH value at which the surface charge is zero is called the point of zero charge (PZC) of the mineral, and the pH value where the zeta potential, defined as the potential at the shear plane of the Stern layer, is zero is known as the isoelectric point (IEP).

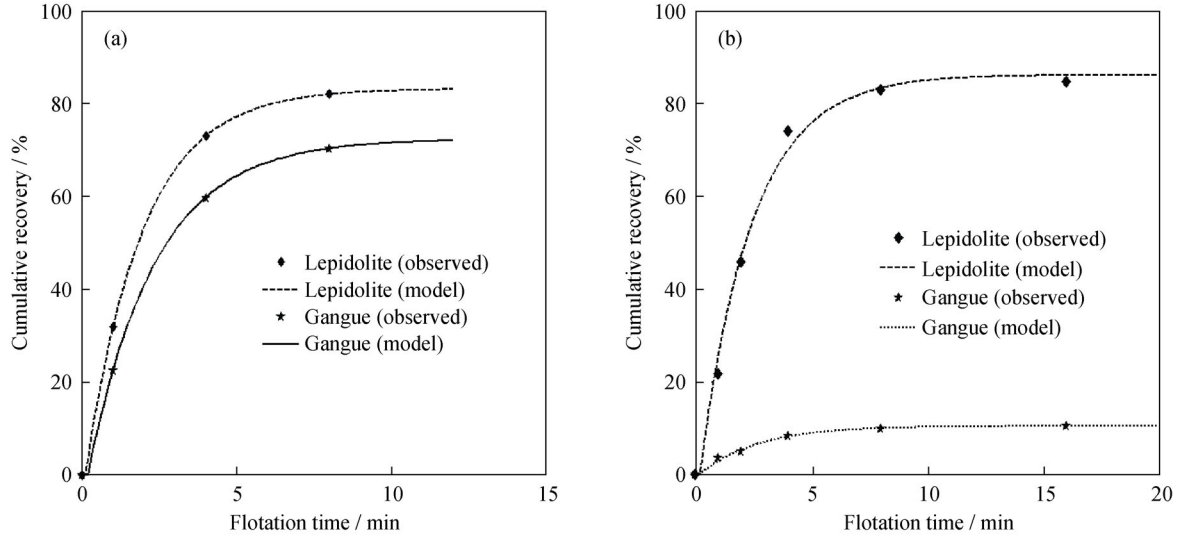

Fig. 5. Cumulative recovery experimentally observed and predicted by the model versus flotation time: (a) Test 3; (b) Test 4.

At pH values less than the PZC/IEP, the surface charge/potential zeta is positive. The PZC/IEP values for several minerals, especially quartz (ranging from 2 to 3.7), have been reported in Ref. [29]. No values have been reported for lepidolite; however, to ensure selective adsorption of cationic collector molecules, we expect that, in this specific case, its PZC/IEP is sufficiently low on the basis of the values of quartz.

Given the average content of lithium and rubidium in the floated fractions, concentrates only 1.05 and 1.28 times richer than the feed were obtained (cumulative recoveries of 71.54% for lithium and 89.59% for rubidium), which, in combination with the low lithium and rubidium contents, demonstrates weak selectivity. The non-floated fraction contained 0.91wt% Li and 0.25wt% Rb. Recoveries estimated through the kinetic model appear to perfectly fit the results obtained experimentally for both mineral groups, as shown in Fig. 5(a).

Test 4 is considered the most complete because incremental concentrates were collected for a larger number of time intervals. This test is characterized by high selectivity, as patent in Fig. 5(b). The selectivity was evaluated by the separation efficiency function, which reached its maximum value for a flotation time of approximately 9–10 min. Moreover, for a flotation time of 8 min, the lepidolite recovery already exceeded 80%. With respect to the average contents of lithium and rubidium in the floated fractions, concentrates 1.78 and 1.54 times richer than the feed were obtained. The cumulative recovery in the floated fraction was 81.29% for lithium and 71.05% for rubidium. The non-floated fraction contained 0.37wt% Li and 0.08wt% Rb.

According to data presented in Table 2, the desliming operation removed 9.5wt% of material, with lithium losses totaling 4%. The lithium content of the final rejected fraction was less than 0.4wt%, and the total losses were less than 2%, which is considered acceptable. As apparent in Fig. 5, the adjusted kinetic model well fit the experimental recovery values.

5.1. Results of the adjusted parameters of the kinetic model

Results of the adjusted parameters of the kinetic models for all the tests performed are shown in Table 3. The optimum flotation time (t_{opt}), the times required to reach 95% and 99% of the maximum separation efficiency function (t_{95} and t_{99}, respectively), the optimum value of the separation efficiency function (SE(t_{opt})), when applicable, and the difference of the ultimate/limit recoveries ($R_{\infty,M} - R_{\infty,G}$) are summarized in Table 4.

Table 3. Results of the adjusted parameters of the kinetic model

Test No.	Mineral group	R_∞ / %	k / min^{-1}	b / min	Sum of squares of residues (SQR)
1	Lepidolite	100.00	0.20	0.20	38.46
	Gangue minerals	22.22	0.32	0.20	15.65
2	Lepidolite	100.00	0.12	0.20	324.22
	Gangue minerals	100.00	0.01	0.20	5.24
3	Lepidolite	82.54	0.59	0.19	0.92
	Gangue minerals	72.47	0.46	0.19	0
4	Lepidolite	86.29	0.44	0.20	35.68
	Gangue minerals	10.35	0.40	0.20	0.69

Table 4. Optimum flotation time, t_{opt}, time t_{95} and t_{99}, SE(t_{opt}), and $R_{\infty,M} - R_{\infty,G}$

Test No.	t_{opt} / min	t_{95} / min	t_{99} / min	SE(t_{opt}) / %	($R_{\infty,M} - R_{\infty,G}$) / %
1	−8.8[#]	16.2	24.4	—	77.8
2	21.4	15.1	19.0	73.1	0
3	3.6	1.8	1.9	12.7	10.9
4	58.9	6.9	10.5	75.9	75.9

Note: [#]The negative value is the result of the inequality $k_M < k_G$.

The separation efficiency curves obtained for all flotation tests performed are shown in Figs. 6(a)–6(d). To highlight the main features of the separation efficiency curves, we expanded the investigated flotation time range to 30 min. The t_{opt}, t_{95}, and t_{99} are also presented. The t_{opt} is not presented in the case of Test 1 (Fig. 6(a)) because the computed value is negative; it is not presented in the case of Test 4 (Fig. 6(d)) because the optimal value is much greater than 30 min.

As evident from Fig. 6, the alternative flotation time, t_{95} and t_{99}, are more reasonable estimations of the near-optimum flotation time, except in the case of Test 3 (Fig. 6(c)). On the basis of the maximum values of SE(t_{opt}) and/or $R_{\infty,M} - R_{\infty,G}$, Test 3 (Fig. 6(c)) is the least selective concentration test, as expected on the basis of the recovery curves for lepidolite mineral and gangue groups. Flotation Test 4 (Fig. 6(d)) was the most successful test performed, with the best value of the separation efficiency function achieved for a near-optimum flotation time between 6.9 and 10.5 min (average value of 9 min).

5.2. Results of the lithium and rubidium contents

According to Refs. [33–34], the occurrence of rubidium and cesium in lepidolite can be explained through the

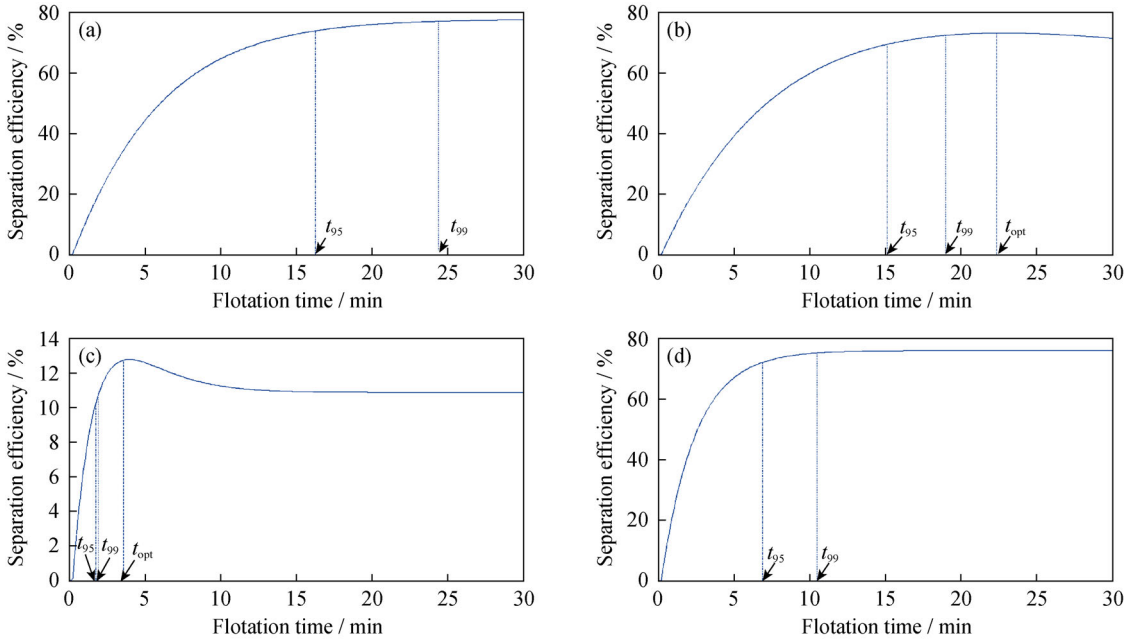

Fig. 6. Separation efficiency as a function of flotation time: (a) Test 1; (b) Test 2; (c) Test 3; (d) Test 4.

isomorphous replacement of potassium. Consequently, Rb is a common byproduct of the processing of lepidolite, which is found in just a few zoned pegmatites around the world [35–36]. Moreover, a small quantity of rubidium is always associated with potassium in this primary crystalline rock [37]. The isomorphic substitution of K by Rb is also an important issue in the ore treatment process. According to Ref. [24], the flotation properties of lepidolite that contains rubidium are different from that of pure lepidolite and the maximum recovery of rubidium from lepidolite is achieved at pH 2.5 using acetate amine (Armac T).

The rubidium and lithium recoveries obtained in the flotation tests are shown in Figs. 7(a)–7(d). In general, the distributions of lithium and rubidium during the flotation and in the non-floated fraction, in all tests, appear to exhibit the same pattern. This result is in accordance with the fact that the bearing mineral of both elements is the same — in this case, lepidolite — because the raw feed ore does not contain K feldspars.

The Li and Rb contents and Li/Rb ratio were relatively constant in all tests performed. Better concentrate results were obtained in the flotation tests for Li (2.50wt%–2.82wt%), Rb (0.52wt%–0.68wt%), and the Li/Rb ratio (4.40–4.92). These values could be considered a geochemical signature of Gonçalo-Seixo Amarelo's lepidolites. The variations associated to the measured values are attributed to analytical limitations and to different proportions of lepidolite versus gangue minerals (quartz and albite).

A similar rubidium content in lepidolite has been reported by Kennard and Rambo [33], who studied the occurrence of rubidium, gallium, and thallium in lepidolite from Pala, California; they reported a rubidium content of 0.67%. Nevertheless, because isomorphous substitutions can vary, the rubidium content is also variable. The contents of rubidium and lithium in a lepidolite concentrate obtained from the BOAM mine (Gyeongsangbuk-do, Korea) and used in a study by Luong *et al.* [37] were 1.43% Rb and 2.55% Li. The same authors studied lepidolite ore from this mine, which they concentrated by hand picking [38]; its rubidium and lithium contents were 0.74% and 1.79%, respectively. Lepidolite from Jiangxi Province (China) was studied and was observed to contain 1.79% Li and 1.21% Rb [39–40].

6. Conclusions

The kinetics of the froth flotation of a lepidolite ore was studied; the following main conclusions are herein reported.

(1) A modified kinetic model for lepidolite flotation process was employed, including a non-negative correction factor for the delay time; in general, a good-to-excellent fitting to the experimental data was obtained.

(2) Two new more reasonable and robust estimations of the near-optimum flotation time are proposed: the flotation time, t_{95} and t_{99}, required to reach 95% and 99% of the maximum separation efficiency function, respectively. These estimations were observed to be much more satisfactory than the usually employed optimum flotation time based on the maximum selectivity difference, which may be sensitive to small uncertainties in the estimated rate constants.

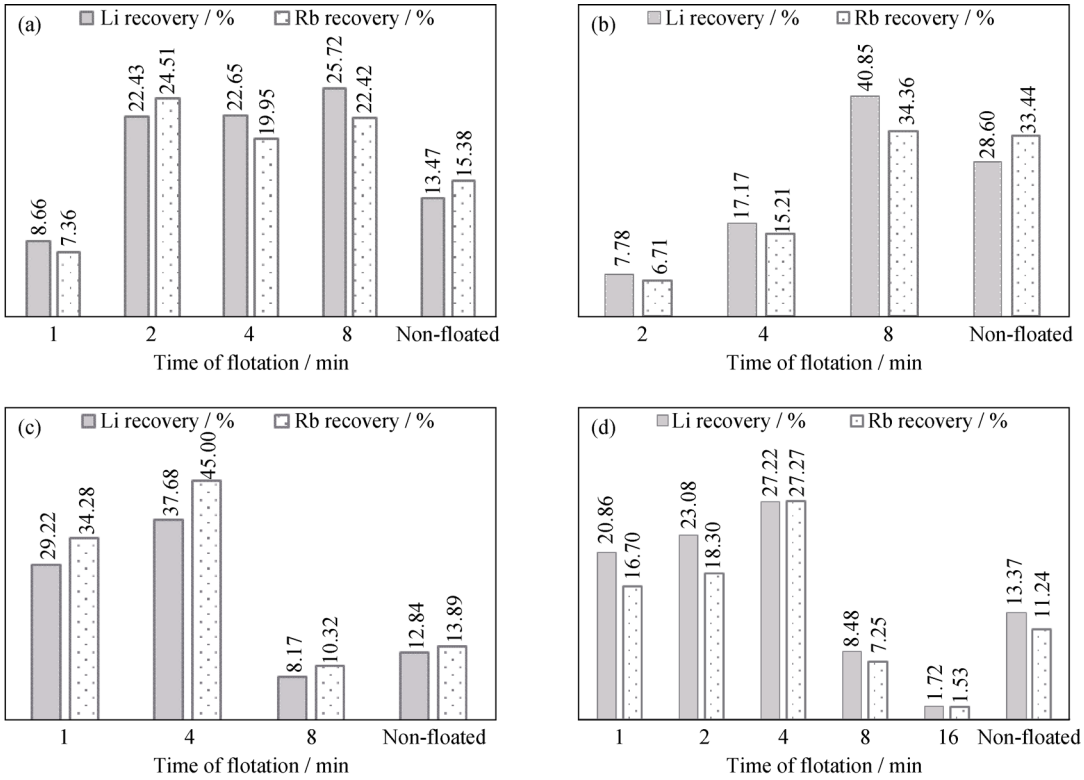

Fig. 7. Results of the rubidium and lithium recoveries obtained in the flotation tests: (a) Test 1; (b) Test 2; (c) Test 3; (d) Test 4.

(3) In the case of the most succeeded flotation test, Test 4, a near-optimum flotation time is a value between 6.9 and 10.5 min. The (adjustable) operating conditions are a pulp pH value equal to 3, a collector dosage of 350 $g \cdot t^{-1}$, and a flotation time of about 9 min. By contrast, the least selective flotation test was Test 3, with a pulp pH value of approximately 7–8.

(4) The high selectivity in the flotation of lepidolite obtained using both collectors at pH 3 was in agreement with the performance of cationic collectors in acidic media. The use of the collector Armeen 12D presented some limitations in this study because it is not soluble in water. Moreover, its application as an ethyl alcohol solution may be detrimental to froth control.

(5) The distributions of lithium and rubidium during the flotation time and in the non-floated fraction appear to exhibit the same patterns in the different tests, indicating the presence of both elements in the mineral structure.

Acknowledgements

The author N. Vieceli acknowledges the doctorate grant ref. 9244/13-1 supplied by Coordenação de Aperfeiçoamento de Pessoal de Nível Superior - CAPES Foundation, Ministry of Education of Brazil. The authors are very grateful to the Cyetc and Akzo Nobel companies, who kindly provided samples of flotation reagents, and to Felmica Minerais Industriais, S.A., for kindly providing the lepidolite ore.

References

[1] F. Hernáinz and M. Calero, Froth flotation: kinetic models based on chemical analogy, *Chem. Eng. Process*., 40(2001), p. 269.

[2] J.L.R. Bahena, A.L. Valdivieso, E.V. Manlapig, and J.P. Franzidis, Optimization of flotation circuits by modelling and simulations, [in] *Proceedings of 2006 China-Mexico Workshop on Minerals Particle Technology*, San Luíz Patosi, 2006.

[3] T.T. Hien-Dinh, V.T. Luong, R. Gieré, and T. Tran, Extraction of lithium from lepidolite via iron sulphide roasting and water leaching, *Hydrometallurgy*, 153(2015), p. 154.

[4] Z.W. Zhao, X.F. Si, X.H. Liu, L.H. He, and X.X. Liang, Li extraction from high Mg/Li ratio brine with $LiFePO_4/FePO_4$ as electrode materials, *Hydrometallurgy*, 133(2013), p. 75.

[5] P. Meshram, B.D. Pandey, and T.R. Mankhand, Extraction of lithium from primary and secondary sources by pre-treatment, leaching and separation: A comprehensive review, *Hydrometallurgy*, 150(2014), p. 192.

[6] I. Kunasz, Lithium, [in] *Industrial and Mineral Rocks*, 7th Ed., Society of Mining, Metallurgy, and Exploration, Inc., Littleton, 2006, p. 599.

[7] M.M.A. Amarante, J.A. Noronha, A.M. Botelho de Sousa,

and M.R. Machado Leite, Processamento tecnológico dos minérios de lítio: Alguns casos de estudo em Portugal, [in] *Valorização de Pegmatitos Litiníferos*, DGEG/LNEG/ADI/CYTED, Lisboa, 2011, p. 43.

[8] A. Moura and J.L. Velho, *Recursos Geológicos de Portugal*, Palimage, Coimbra, 2011.

[9] J.M.F. Ramos, Aplitopegmatitos com mineralizações de metais raros de Seixo Amarelo–Gonçalo. O recurso Geológico, [in] *Ciências Geológicas*: *Ensino*, *Investigação e sua História*, Associação Portuguesa de Geólogos, Lisboa, 2010, p. 121.

[10] A. Lima, R. Vieira, T. Martins, and F. Noronha, As fontes de lítio em Portugal, [in] *Portugal Mineral*, 3rd Ed., Associação Nacional da Indústria Extractiva e Transformadora - ANIET, Porto, 2011, p. 60.

[11] S. Kelebek and B. Nanthakumar, Characterization of stockpile oxidation of pentlandite and pyrrhotite through kinetic analysis of their flotation, *Int. J. Miner. Process.*, 84(2007), No. 1-4, p. 69.

[12] A.J. Lynch, N.W. Johnson, E.V. Manlaping, and C.G. Thome, *Mineral and Coal Flotation Circuits*: *Their Simulation and Control*, Elsevier Science Ltd, New York, 1981.

[13] X.M. Yuan, B.I. Palsson, and K.S.E. Forssberg, Statistical interpretation of flotation kinetics for a complex sulphide ore, *Miner. Eng.*, 9(1996), No. 4, p. 429.

[14] R.R. Klimpel, *Selection of Chemical Reagents for Flotation*, 2nd Ed., Society of Mining Engineers, Littleton, 1980.

[15] D.F. Kelsall, Application of probability in the assessment of flotation systems, *Trans. Inst. Min. Metall.*, 70(1961), No. 4, p. 191.

[16] A. Jowett, Resolution of flotation recovery curves by a differential plot method, *Trans. Inst. Min. Metall.*, 85(1974), p. C263.

[17] M. Polat and S. Chandler, First-order flotation kinetics models and methods for estimation of the true distribution of flotation rate constants, *Int. J. Miner. Process*., 58(2000), p. 145.

[18] A.L. Mular and R.B. Bhappu, *Mineral Processing Plant Design*, 2nd ed., Society of Mining Engineers (SME) of The American Institute of Mining, Metallurgical and Petroleum Engineers Inc., New York, 1980.

[19] Cytec Industries Inc., *Mining Chemicals Handbook*, Cytec Industries Inc., New Jersey, 2002.

[20] A.P. Chaves, L.S.L. Filho, and P.F.A. Braga, Flotação, [in] *Tratamento de Minérios*, 5th Ed., Centro de Tecnologia Mineral - CETEM, Rio de Janeiro, 2010, p. 465.

[21] T.N. Wills and B.A. Munn, *Will's Mineral Processing Technology*, 7th Ed., Elsevier Science & Technology Book, Oxford, 2006.

[22] F. Concha and E.R. Almendra, Settling velocities of particulate systems: 1. Settling velocities of individual spherical particles, *Int. J. Miner. Process*., 5(1979), No. 4, p. 349.

[23] F. Concha and E.R. Almendra, Settling velocities of particulate systems: 2. Settling velocities of suspensions of spherical particles, *Int. J. Miner. Process.*, 6(1979), No. 1, p. 31.

[24] S.M. Bulatovic, *Handbook of Flotation Reagents*: *Chemistry*, *Theory and Practice*, Vol. 3, Elsevier, Amsterdam, Oxford, 2015.

[25] G.E. Agar, The optimization of flotation circuit design from laboratory rate data, [in] *XVth International Mineral Processing Congress*, Vol. 2, Cannes, 1985, p. 100.

[26] R. Samková, Recovering lithium mica from the waste after mining Sn–W ores through the use of flotation, *GeoSci. Eng.*, LV(2009), No. 1, p. 33.

[27] Y.L. Liu and J. Liu, The flotation process of lepidolite in Jiangxi Province in China, *Adv. Mater. Res.*, 1033-1034(2014), p. 1309.

[28] C.G.A. Nogueira, *Extracção de Lítio de Recursos Nacionais*, Technical Report, LNETI, Lisboa, 1991.

[29] S.M. Bulatovic, *Handbook of Flotation Reagents*: *Chemistry*, *Theory and Practice*, Vol. 1, Elsevier Science, Amsterdam, 2007.

[30] E.G. Kelly and D.J. Spottiswood, *Introduction to Mineral Processing*, John Wiley & Sons, New York, 1982.

[31] D.W. Fuerstenau and S. Raghavan, Some aspects of the thermodynamics of flotation, [in] *Flotation*, A.M. Gaudin Memorial and M.C. Fuerstenau, eds., AIME, New York, 1976.

[32] S.R. Ramachandra, *Surface of Chemistry of Froth Flotation*, 2nd ed., Springer Science + Business Media, New York, 2004.

[33] T.G. Kennard and A.I. Rambo, Occurrence of rubidium, gallium and thallium in lepidolite from Pala, California, *Am. Mineral.*, 18(1933), No. 10, p. 454.

[34] W.C. Butterman and R.G. Reese Jr, *Mineral Commodity Profiles*: *Rubidium*, Open-File Report, 03-045, U.S. Geological Survey, 2003.

[35] Royal Society of Chemistry. *Chemistry in its Element*: *Rubidium*. [2015-05-25] http://www.rsc.org/chemistryworld/podcast/interactive_periodic_table_transcripts/rubidium.asp.

[36] S.F. Singer and S.S. Singer, *Industrial Ceramics*, Springer Science + Business Media, Netherlands, 1963.

[37] V.T. Luong, D.J. Kang, J.W. An, M.J. Kim, and T. Tran, Factors affecting the extraction of lithium from lepidolite, *Hydrometallurgy*, 134-135(2013), p. 54.

[38] V.T. Luong, D.J. Kang, D.W. An, D.A. Dao, M.J. Kim, and T. Tran, Iron sulphate roasting for extraction of lithium from lepidolite, *Hydrometallurgy*, 141(2014), p. 8.

[39] Q.X. Yan, X.H. Li, Z.X. Wang, J.X. Wang, H.J. Guo, Q.Y. Hu, W.J. Peng, and X.F. Wu, Extraction of lithium from lepidolite using chlorination roasting-water leaching process, *Tran. Nonferrous Met. Soc. China*, 22(2012), No. 7, p. 1753.

[40] Q.X. Yan, X.H. Li, Z.X. Wang, X.F. Wu, H.J. Guo, Q.Y. Hu, W.J. Peng, and J.X. Wang, Extraction of valuable metals from lepidolite, *Hydrometallurgy*, 117-118(2012), p. 116.